

Oxorhenium(V) Complexes with the Non-Sulfur-Containing Amino Acid Histidine

Christian Tessier,[†] Fernande D. Rochon,[‡] and André L. Beauchamp*[†]

Département de chimie, Université de Montréal, C.P. 6128, Succ. Centre-ville, Montréal, Québec, Canada, H3C 3J7, and Département de chimie, Université du Québec à Montréal, C.P. 8888, Succ. Centre-ville, Montréal, Québec, Canada, H3C 3P8

Received June 20, 2002

Equivalent amounts of $\text{ReOX}_3(\text{OPPh}_3)(\text{Me}_2\text{S})$ (where $\text{X} = \text{Cl}, \text{Br}$) and L-histidine (L-hisH) in acetonitrile yield $\text{ReOX}_2(\text{L-his})$, in which the amino acid monoanion is N,N,O-tridentate. X-ray diffraction work on both compounds shows that the three donors occupy a face in a distorted octahedron and the carboxylate oxygen is coordinated trans to the $\text{Re}=\text{O}$ bond. The 2:1 complex $[\text{ReO}(\text{L-his})_2]\text{I}$ is obtained by reacting 2 equiv of L-histidine with $\text{ReO}_2\text{I}(\text{PPh}_3)_2$ in methanol in the presence of NaOCH_3 . ^1H NMR spectroscopy indicates that these complexes contain one N,N,O-tridentate histidine anion coordinated as above and one N,N-bidentate histidine anion, whose carboxylate group is free. By refluxing $\text{ReOX}_2(\text{L-his})$ in methanol, the carboxylic groups esterify and two octahedral units condense into an oxo-bridged dinuclear complex $\{\text{ReOX}_2(\text{L-hisMe})\}_2\text{O}$ containing N,N-bidentate histidine methyl ester. The $\text{O}=\text{Re}-\text{O}-\text{Re}=\text{O}$ backbone is approximately linear, and the two $\text{ReOX}_2(\text{L-hisMe})$ units are related by a 2-fold axis through the central oxygen. Crystals of $\{\text{ReOBr}_2(\text{L-hisMe})\}_2\text{O}$ consist of an ordered phase containing two of the possible diastereoisomers in a 1:1 ratio. ^1H NMR spectra of these crystals include two sets of signals, consistent with the presence of two isomers with C_2 symmetry, and the spectra of the nonrecrystallized material confirm that these are the only two isomers formed.

Introduction

The radioactive $^{99\text{m}}\text{Tc}$ isotope is the most widely used imaging agent in nuclear medicine.^{1–3} Since no stable isotopes are available for this element, rhenium was largely used as a model to develop its chemistry. However, in the past decade, rhenium has been attracting increasing attention for itself, because radioactive Re nuclei have shown promising results as radiotherapeutic agents.⁴

Specific targeting is achieved by adjusting the environment of the Tc or Re centers. Most of the currently FDA approved Tc imaging agents are so-called *technetium essentials*. In such systems, the radionucleus is coordinated with relatively simple ligands not necessarily found in normal biological

systems and the biodistribution depends on the overall physical and chemical properties of the complexes. To improve specificity, biologically active molecules (BAM), such as receptor agonist or antagonist or monoclonal antibodies,¹ are being considered as carriers. These molecules are labeled with $^{99\text{m}}\text{Tc}$ either by binding the radionucleus directly to the BAM or by anchoring it to the BAM via a bifunctional coupling agent (BFCA).³ Amino acids and small peptides are promising ligands to bind Tc or Re, since they can be considered for any of the above strategies.^{1,5,6} A significant advantage of using small peptides as BFCA lies in the easy attachment of the chelating agent via solid-phase peptide synthesis.

Several amino acid complexes of rhenium in low oxidation states have been reported.^{7–10} Recently, from the versatile starting material $[\text{NEt}_4][\text{fac-ReCl}_3(\text{CO})_3]$, Alberto and co-

* Corresponding author. Tel: (514) 343-6446. Fax: (514) 343-7586. E-mail: beauchamp@chimie.umontreal.ca.

[†] Université de Montréal.

[‡] Université du Québec à Montréal.

(1) Dilworth, J. R.; Parrott, S. J. *Chem. Soc. Rev.* **1998**, 27, 43–55.

(2) Jurisson, S. S.; Lydon, J. D. *Chem. Rev.* **1999**, 99, 2205–2218.

(3) Liu, S.; Edwards, D. S. *Chem. Rev.* **1999**, 99, 2235–2268.

(4) Nicolini, M.; Mazzi, U. *Technetium, Rhenium and Other Metals in Chemistry and Nuclear Medicine*; Servizi Grafici Editoriali: Padova, Italia, 1999.

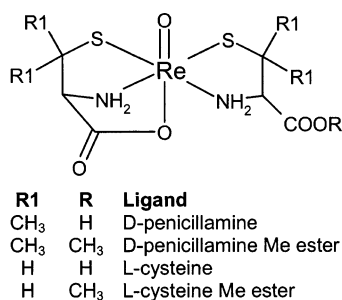
(5) Fritzberg, A. R.; Kasina, S.; Eshima, D.; Johnson, D. L. *J. Nucl. Med.* **1986**, 27, 111–116.

(6) Alberto, R.; Schibli, R.; Waibel, R.; Abram, U.; Schubiger, A. P. *Coord. Chem. Rev.* **1999**, 192, 901–919.

(7) Sladkov, A. M.; Vasneva, N. A.; Johansson, A. A.; Derunov, V. V. *Inorg. Chim. Acta* **1977**, 25, L97–L99.

(8) Ioganson, A. A.; Derunov, V. V. *Koord. Khim.* **1980**, 57, 1707–1714.

Chart 1



workers⁶ obtained the tridentate histidine complex $\text{Re}(\text{CO})_3\text{-(his-}N,N,O\text{)}$, whose characterization has been briefly described. (To follow the replacement of the acidic proton of histidine, the un-ionized molecule is represented as hisH, the monoanion by his, and the methyl ester by hisMe. A similar convention is applied to the amino acids cysteine (cysH₂) and penicillamine (penH₂) discussed later.) Less is known about the higher oxidation states.^{11,12} Oxorhenium(V) monomers were prepared with cysteine, penicillamine,^{13–15} and their methyl esters.^{16–18} Besides the $\text{Re}=\text{O}$ moiety, these compounds contain two ligands, one tridentate-S,N,O and the other bidentate-S,N (Chart 1).

Most of the Tc(V)-labeled peptides contain a thiolate sulfur donor.³ Thiol-containing peptides present a serious inconvenience in radiopharmacy: they are unstable in the free form and must be protected during storage, leading to a reduced labeling efficiency and specific activity of the Tc-labeled biomolecule. For an N₄ donor set, such as the Gly-Ala-Gly-Gly tetrapeptide,¹⁹ this protection step is unnecessary. We are considering histidine-containing peptides, which can be stored in a nonprotected form, as alternative ways of labeling the biological molecules with Tc or Re radionuclei. The present paper deals with the first step of this study, namely, the reactivity of rhenium(V) with histidine. The compounds described here are the first rhenium(V) complexes to be prepared and fully characterized with a non-sulfur-containing amino acid. (Some of the results reported here were described in a very preliminary form in a conference proceeding.²⁰)

- (9) Kovalev, Y. G.; Ioganson, A. A. *Zh. Obshch. Khim.* **1987**, *57*, 1939–1943.
- (10) Derunov, V. V.; Konstantinov, P. A.; Vasneva, N. A.; Sladkov, A. M.; Ioganson, A. A. *Dokl. Akad. Nauk SSSR* **1978**, *239*, 1107–1109.
- (11) Romiti, P.; Freni, M.; D'Alfonso, G. *Gazz. Chim. Ital.* **1977**, *107*, 497–498.
- (12) Arkowska, A.; Wojciechowski, W. *Bull. Acad. Pol. Sci., Ser. Sci. Chim.* **1979**, *27*, 963–972.
- (13) Johnson, D. L.; Fritzberg, A. R.; Hawkins, B. L.; Kasina, S.; Eshima, D. *Inorg. Chem.* **1984**, *23*, 4204–4207.
- (14) Kirsch, S.; Noll, B.; Scheller, D.; Klostermann, K.; Leibnitz, P.; Spies, H.; Johannsen, B. *Forschungszent. Rossendorf* **1996**, *FZR-122*, 110–114.
- (15) Chatterjee, M.; Achari, B.; Das, S.; Banerjee, R.; Chakrabarti, C.; Dattagupta, J. K.; Banerjee, S. *Inorg. Chem.* **1998**, *37*, 5424–5430.
- (16) Kirsch, S.; Noll, B.; Spies, H.; Leibnitz, P.; Scheller, D.; Johannsen, B. *Forschungszent. Rossendorf* **1997**, *FZR-165*, 50–55.
- (17) Kirsch, S.; Noll, B.; Spies, H.; Leibnitz, P.; Scheller, D.; Krueger, T.; Johannsen, B. *J. Chem. Soc., Dalton Trans.* **1998**, 455–460.
- (18) Kirsch, S.; Jankowsky, R.; Leibnitz, P.; Spies, H.; Johannsen, B. *J. Biol. Inorg. Chem.* **1999**, *4*, 48–55.
- (19) Benhaim, S.; Kahn, D.; Weiner, G. J.; Madsen, M. T.; Waxman, A. D.; Williams, C. M.; Clarkepearson, D. L.; Coleman, R. E.; Maguire, R. T. *Nucl. Med. Biol.* **1994**, *21*, 131–142.

Experimental Section

Reactants and Methods. KReO_4 (Aldrich), the amino acids (Aldrich), the solvents, and all other chemicals were used as received. Deuterated solvents were purchased from CDN Isotopes. The starting materials $\text{ReOX}_3(\text{OPPh}_3)(\text{Me}_2\text{S})$ ^{21,22} ($X = \text{Cl}$ or Br) and $\text{ReIO}_2(\text{PPh}_3)_2$ ²³ were prepared following published procedures.

¹H NMR spectra were recorded at 300 MHz on a Bruker AMX-300 spectrometer in deuterated methanol or DMSO. The solvent signals ($\delta = 3.31$ and 2.50 ppm for CD_3OD and $(\text{CD}_3)_2\text{SO}$, respectively) were used as internal references. IR spectra were recorded from 4000 to 450 cm^{-1} on a Perkin-Elmer 1750 FTIR spectrometer as KBr pellets. Elemental analyses were performed at the Laboratoire d'analyse élémentaire de l'Université de Montréal. Mass spectra were recorded in the FAB^+ mode as nitrobenzyl alcohol solutions at the Centre Régional de Spectrométrie de Masse de l'Université de Montréal.

Preparative Work. The ¹H NMR and IR data for the complexes are provided in Tables 2, 3, and S-1 (Supporting Information).

$\text{ReOCl}_2(\text{L-his-}N,N,O)$ (1). $\text{ReOCl}_3(\text{OPPh}_3)(\text{Me}_2\text{S})$ (65 mg, 0.10 mmol) is suspended in acetonitrile (15 mL), L-hisH (15.8 mg, 0.10 mmol) is added, and the green suspension is refluxed for 3 h. The light-blue solution is filtered to remove the small amount of light-green precipitate, and the solution is evaporated to dryness. The oily residue is dissolved in a minimum of acetonitrile and precipitated with benzene. The solid is washed with benzene and dried in vacuo. Lattice benzene is not completely removed by overnight pumping. Yield: 56%. Anal. Calcd for $\text{ReCl}_2\text{O}_3\text{N}_3\text{C}_6\text{H}_8 \cdot \frac{1}{2}\text{C}_6\text{H}_6$: C 18.00, H 1.98, N 9.69. Found: C 18.04, H 1.87, N 9.98. $\text{FAB}^+\text{-MS}$: $m/z = 428$ ($M + H^+$).

$\text{ReOBr}_2(\text{L-his-}N,N,O)$ (2). The above procedure for $\text{ReOCl}_2(\text{L-his})$ is applied starting with $\text{ReOBr}_3(\text{OPPh}_3)(\text{Me}_2\text{S})$. No light-green precipitate appears. Yield: 49%. Anal. Calcd for $\text{ReBr}_2\text{O}_3\text{N}_3\text{C}_6\text{H}_8 \cdot \frac{1}{3}\text{C}_6\text{H}_6$: C 17.72, H 1.86, N 7.75. Found: C 17.72, H 1.82, N 7.47. $\text{FAB}^+\text{-MS}$: $m/z = 518$ ($M + H^+$).

$[\text{ReO}(\text{L-his-}N,N,O)(\text{L-his-}N,N)]$ (3). L-hisH (31.6 mg, 0.20 mmol) and CH_3ONa (0.20 mL of a 3% solution in methanol, 0.10 mmol) are dissolved in methanol (20 mL) with heating. $\text{ReIO}_2(\text{PPh}_3)_2$ (88.5 mg, 0.10 mmol) is then added, and the solution is refluxed. The purple suspension turns green after 5 min, and refluxing is continued for 90 min. The solution is evaporated to dryness without heating, affording an oily residue. Dissolution in a minimum of methanol and precipitation with ether yields a green powder, which is washed with ether and dried in vacuo. Yield: 73%. Anal. Calcd for $\text{ReO}_5\text{N}_6\text{C}_{12}\text{H}_{16} \cdot \text{CH}_3\text{OH}$: C 23.32, H 3.01, N 12.55. Found: C 23.46, H 3.04, N 12.60. $\text{FAB}^+\text{-MS}$: $m/z = 512$ (M^+).

$[\{\text{OReCl}_2(\text{L-hisMe})\}_2(\mu\text{-O})]$ (4). $\text{ReOCl}_2(\text{L-his})$ is refluxed in methanol for 20 h, affording a light-green precipitate, which is filtered off, washed with methanol, and dried in vacuo. Yield: 27%. Anal. Calcd for $\text{Re}_2\text{Cl}_4\text{O}_7\text{N}_6\text{C}_{14}\text{H}_{22} \cdot \frac{1}{2}\text{CH}_3\text{OH}$: C 19.00, H 2.64, N 9.17. Found: C 19.05, H 2.63, N 9.16.

A small crystalline sample of the corresponding bromo analogue was obtained by the same method and used for an X-ray diffraction study.

Crystallographic Measurements and Structure Determination. Blue crystals of $\text{ReOCl}_2(\text{L-his}) \cdot \frac{1}{2}\text{H}_2\text{O}$ (1) and $\text{ReOBr}_2(\text{L-his}) \cdot$

- (20) Tessier, C.; Beauchamp, A. L.; Rochon, F. D. *J. Inorg. Biochem.* **2001**, *85*, 77–78.
- (21) Grove, D. E.; Wilkinson, G. *J. Chem. Soc. A* **1966**, 1224–1230.
- (22) Bryan, J. C.; Stenkamp, R. E.; Tulip, T. H.; Mayer, J. M. *Inorg. Chem.* **1987**, *26*, 2283–2288.
- (23) Ciani, G. F.; D'Alfonso, G.; Romiti, P.; Sironi, A.; Freni, M. *Inorg. Chim. Acta* **1983**, *72*, 29–37.

Table 1. Crystallographic Data

	1	2	4
chem formula	ReOCl ₂ (L-his) [•] 1/2H ₂ O	ReOBr ₂ (L-his) [•] 1/2H ₂ O	{ORe(L-hisMe)Br ₂ } ₂ O [•] 1/2CH ₃ OH
<i>M_w</i>	C ₆ H ₉ Cl ₂ N ₃ O _{3.5} Re 436.26	C ₆ H ₉ Br ₂ N ₃ O _{3.5} Re 525.18	C _{14.5} H ₂₄ Br ₄ N ₆ O _{7.5} Re ₂ 1094.44
space group	<i>P</i> 4 ₁ 2 ₁ 2 (No. 76)	<i>P</i> 4 ₁ 2 ₁ 2 (No. 76)	<i>I</i> 2 (No. 5)
<i>a</i> (Å)	12.097(9)	12.250(2)	15.349(3)
<i>b</i> (Å)			9.686(2)
<i>c</i> (Å)	15.843(11)	16.020(5)	18.658(4)
β (deg)			102.74(3)
vol (Å ³)	2318(2)	2404.0(9)	2705.6(10)
<i>Z</i>	8	8	4
ρ_{calcd} (g cm ⁻³)	2.500	2.902	2.687
μ (mm ⁻¹)	24.778	16.754	14.894
λ (Å)	1.54178	0.71073	0.71073
cryst size (mm)	0.54 × 0.47 × 0.21	0.38 × 0.31 × 0.16	0.12 × 0.11 × 0.03
measd reflns	21779	4882	13077
indep reflns (<i>R</i> _{int})	2208 (0.188)	2349 (0.073)	6230 (0.089)
ranges of <i>h</i> , <i>k</i> , <i>l</i>	-14 ≤ <i>h</i> ≤ 14 -14 ≤ <i>k</i> ≤ 14 -19 ≤ <i>l</i> ≤ 19	-15 ≤ <i>h</i> ≤ 0 -15 ≤ <i>k</i> ≤ 0 -19 ≤ <i>l</i> ≤ 15	-19 ≤ <i>h</i> ≤ 19 -12 ≤ <i>k</i> ≤ 12 -24 ≤ <i>l</i> ≤ 24
<i>R</i> 1 ^a	0.0332	0.0414	0.0489
w <i>R</i> 2 ^b	0.0891	0.0739	0.0940
<i>S</i> ^c	1.087	1.027	0.994
Flack	-0.04(3)	-0.03(3)	0.03(3)

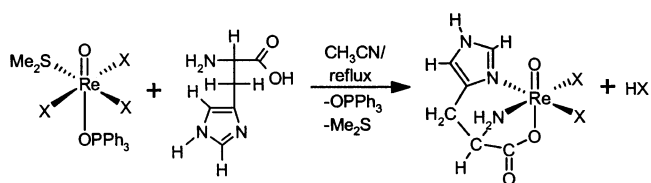
^a For data with $I > 2\sigma(I)$: $R1 = \sum(|F_o| - |F_c|)/\sum|F_o|$. ^b All data: $wR2 = [\sum(w(F_o^2 - F_c^2)^2)/\sum(w(F_o^2)^2)]^{1/2}$. ^c $S = [\sum[w(F_o^2 - F_c^2)]/(N_{\text{reflins}} - N_{\text{params}})]^{1/2}$.

1/2H₂O (**2**) were obtained by recrystallization in acetonitrile, whereas light-green crystals of {ReOBr₂(L-hisMe)}₂O[•]1/2CH₃OH (**4**) precipitated when crystals of **2** dissolved in methanol were left in the refrigerator for 2 weeks.

Crystal **1** was studied on an Enraf-Nonius CAD-4 diffractometer operating with Cu K α radiation. A Bruker P4 diffractometer controlled by the XSCANS²⁴ program with Mo K α radiation was used for **2** and **4**. The intensity data, which were collected at room temperature, were corrected for absorption and for Lorentz and polarization effects. The SHELXTL²⁵ system was used for all calculations and drawings. The coordinates of the Re atoms were determined from a Patterson map, and the positions of all other non-hydrogen atoms were found by the standard Fourier method. The structures were refined on F_o^2 using all reflections. The H atoms were fixed using a riding model with $U_{\text{iso}} = 1.2U_{\text{eq}}$ of the supporting atom (1.5 for methyl or hydroxyl groups). The crystal data are listed in Table 1.

Structure resolution presented no particular problems for **1** and **2**, but **4** required considerable effort. The systematic absences suggested space group *C*2/*c* or *C**c*. Even though these groups were not consistent with the presence of chiral L-histidine, the heavy-atom method in space group *C*2/*c* led to a reasonable unit cell containing four equivalent oxo-bridged {O=ReBr₂(hisMe-*N,N*)}₂O molecules. The central oxo group lay on a crystallographic 2-fold axis that rotated the two O=ReBr₂(hisMe-*N,N*) fragments into one another. After refinement, a few atoms showed relatively large thermal parameters and the methylene carbon of histidine was disordered over two positions, above and below the mean plane through the chelate ring. Since the presence of a chiral ligand was consistent with neither *C*2/*c* nor *C**c*, it was concluded that the true space group should have lower symmetry and that the departure from higher symmetry was produced by a very small amount of electron density, located in the immediate environment of the chiral carbon. This portion would represent too small a contribution to the $h0l$ odd reflections to produce intensities above background

Scheme 1



in this subset of reflections and provide direct evidence that the *c* glide planes were absent. The space group obtained by discarding the inconsistent glide planes and inversion centers is *C*2. Resolution in this space group led to essentially the same structure as above, except that the two molecules related by the inversion center in the *C*2/*c* model became nonequivalent, occupying distinct special positions (*2a* and *2b*) on symmetry-independent 2-fold axes. Again, two peaks occurred in the Fourier map about the methylene carbon of both molecules (C16 and C26). The site consistent with the chirality of L-histidine in the first molecule was selected for C16, whereas no coordinates were initially supplied for C26 in the other molecule. In the next Fourier map, a single peak appeared for C26, corresponding to chirality L. The *C*2 cell ($\beta = 121.68^\circ$) was transformed into the equivalent *I*2 cell ($\beta = 102.74^\circ$) to minimize the correlations due to the large β angle in the least-squares refinement. Nevertheless, great care had to be taken to control the progression of refinement, since high correlations remained between the two independent but very similar molecules. The Flack parameter of 0.03(3) confirmed that the chirality was correct.

Results

Monosubstituted Complexes. Refluxing 1 equiv of histidine with ReOX₃(OPPh₃)(Me₂S) in acetonitrile affords the neutral monosubstituted compounds ReOX₂(L-his-*N,N,O*) (Scheme 1), where X = Cl and Br. The blue complexes are soluble in acetonitrile and isolated by precipitation with benzene. The elemental analysis and the mass spectra (*m/z* and isotopic distribution of the parent peak) are consistent with the above composition, which is confirmed by a crystallographic study (see below) showing that the histidine ligand is tridentate.

(24) XSCANS, X-ray Single-Crystal Analysis Software, PC version 5; Bruker AXS Inc.: Madison, WI, 1995.

(25) SHELXTL, The Complete Software Package for Single-Crystal Structure Determination, release 5.10; Bruker AXS Inc.: Madison, WI, 1997.

Table 2. ^1H NMR Chemical Shifts (ppm) and Coupling Constants (Hz)^a

complex	H ₂	H ₄	H _{6'/6''}	$\Delta\nu^b$	$^2J(\text{H}_{6'}-\text{H}_{6''})$	H ₇	$^3J(\text{H}_{6'/6''}-\text{H}_7)$
L-histidine	7.620 d	6.953 d	3.216 dd; 3.004 dd	64	15.32	3.765 dd	4.09; 8.42
L-His·HCl	8.585 d	7.328 d	3.279; ^c 3.215 ^c	22	15.59	3.915 dd	6.04; 6.93
ReOCl ₂ (L-his)	8.745 d	7.332 d	3.660; ^c 3.612 ^c	15	17.55	4.582 t ^c	4.02; 3.23
ReOBr ₂ (L-his)	8.947 d	7.321 d	3.696; ^c 3.648 ^c	14	17.38	4.485 t ^c	3.90; 3.75
[ReO(L-his) ₂]I	8.678 d	7.259 d	3.532 dd; 3.181 dd	105	14.97	4.679 dd	4.03; 4.86
	8.522 d	7.373 d	3.557 d ^c			4.363 t ^c	3.63 ^d

^a In CD₃OD. ^b $\Delta\nu(\text{H}_{6'}-\text{H}_{6''})$. ^c Second-order signal. Data obtained by refinement with program NUTS.³² ^d J_{average} .

The infrared spectra of the chloro and bromo complexes are almost superimposable. The wavenumbers and partial tentative assignments are provided in Table S-1. The $\nu(\text{Re}=\text{O})$ vibration should produce a strong band at 945–1067 cm⁻¹.²⁶ Strong peaks are indeed observed at 988 and 1008 cm⁻¹, but their assignments are uncertain. Bands due to imidazole vibrations have been identified at 980–990 and 1010–1030 cm⁻¹ for Cr(III) complexes,^{27,28} and at 960–970 and 1020–1030 cm⁻¹ for aqueous solutions of complexes with M²⁺ cations.²⁹ In the present case, the 988 cm⁻¹ component is believed to correspond to a ring mode, whereas the frequency of the $\nu(\text{Re}=\text{O})$ vibration would be 1008 cm⁻¹, similar to the one reported for the [ReOCl₂(OPPh₃)(2,2'-biimidazole)]⁺ cation (1000 cm⁻¹).³⁰ This interpretation would be consistent with the IR spectrum of the [ReO(L-his-*N,N,O*)(L-his-*N,N*)]I complex described herein, which also contains histidine but exhibits no band at ~1008 cm⁻¹. This frequency is slightly high for $\nu(\text{Re}=\text{O})$, but much lower than the one reported for the five-coordinate species [ReOCl₄]⁻ (1067 cm⁻¹).³¹

Upon coordination, the $\nu(\text{N}-\text{H})$ region changes drastically, as the very broad band of free histidine at ~3000 cm⁻¹ splits into sharper components at 3210/3130/3050/2930 cm⁻¹ due to $\nu_{\text{a}}(\text{NH}_2)$, $\nu_{\text{s}}(\text{NH}_2)$, and imidazole $\nu(\text{N}-\text{H})$ motions. The $\delta(\text{NH}_2)$ mode appears as a medium band at ~1590 cm⁻¹, and the twisting vibration produces a medium, slightly broadened feature at 1168 (Cl) or 1182 (Br) cm⁻¹.²⁷ The $\nu_{\text{as}}(\text{CO}_2)$ vibration is readily identified as the very strong and sharp peak at 1690 cm⁻¹, whereas the $\nu_{\text{s}}(\text{CO}_2)$ counterpart is believed to correspond to the medium peak at 1373 cm⁻¹. These displacements in opposite directions with respect to the free carboxylate vibrations (1579 and 1412 cm⁻¹)²⁹ are typical of carboxylate coordination.²⁷ The large shifts observed here suggest the presence of an ester-like carboxylate, whose vibrations are probably better described as $\nu(\text{C}=\text{O})$ and $\nu(\text{C}-\text{O})$. A well-defined medium band at ~597 cm⁻¹ could be due to a deformation mode of the coordinated carboxylate.²⁸ The spectra include a number of vibrations originating from the imidazole ring, but no characteristic

changes that could be used as diagnostic for imidazole coordination were detected.

The NMR data for the complexes and free histidine are listed in Table 2. The protons are numbered according to Chart 2. No signals are observed for the labile N–H protons because of fast exchange with the solvent (CD₃OD). The C₇ chiral carbon makes the H_{6'/6''} protons diastereotopic. In free histidine, the $^2J(\text{H}_{6'}-\text{H}_{6''})$ coupling constant is much smaller than the chemical shift difference, so that a near-first-order spectrum is observed with modifications only in the intensity distribution in the AMX pattern. Upon protonation or coordination, the chemical shift difference becomes smaller, and a second-order ABX pattern is observed. The data given in Table 2 were determined from simulation and refinement with the NUTS program.³² Upon coordination, all signals shift to lower field, which is consistent with a net reduction of electron density in histidine. General downfield shift is not a reliable diagnostic for ligand coordination, since protonation has the same effect. For instance, the aromatic signals are deshielded roughly to the same extent by protonation and coordination. However, the H₇ signal appears to be a valid probe for coordination, since the deshielding is much larger for the complexes than for protonated histidine.

The $^3J(\text{H}_{6'}-\text{H}_7)$ and $^3J(\text{H}_{6''}-\text{H}_7)$ coupling constants are commonly used to provide information on amino acid conformations.³³ Obviously, tridentate coordination to the nonlabile Re center precludes conformational freedom in the present case (see the crystallographic work below), but for future use on less restricted systems, we wanted to verify whether the observed conformation could be predicted from the procedure applicable to free amino acids.

The three rotamers for free histidine are shown in Chart 3, and their populations can be calculated from eqs 1–3a.³³

$$P_{\text{I}} = \frac{{}^3J(\text{H}_{6'}-\text{H}_7) - J_{\text{g}}}{J_{\text{t}} - J_{\text{g}}} \quad (1)$$

$$P_{\text{II}} = \frac{{}^3J(\text{H}_{6''}-\text{H}_7) - J_{\text{g}}}{J_{\text{t}} - J_{\text{g}}} \quad (2)$$

$$P_{\text{III}} = 1 - P_{\text{I}} - P_{\text{II}} \quad (3)$$

$$P_{\text{III}} = 1 - \frac{{}^3J(\text{H}_{6'}-\text{H}_7) + {}^3J(\text{H}_{6''}-\text{H}_7) - 2J_{\text{g}}}{J_{\text{t}} - J_{\text{g}}} \quad (3a)$$

The three populations determined by this method were found

(26) Nugent, W. A.; Mayer, J. M. *Metal-Ligand Multiple Bonds: The Chemistry of Transition Metal Complexes Containing Oxo, Nitrido, Imido, Alkylidene, or Alkylidyne Ligands*; John Wiley & Sons: New York, 1988.

(27) Hoggard, P. E. *Inorg. Chem.* **1981**, *20*, 415–420.

(28) Vicens, M.; Prats, M.; Fiol, J. J.; Terron, A.; Moreno, V. *Inorg. Chim. Acta* **1989**, *158*, 59–68.

(29) Carlson, R. H.; Brown, T. L. *Inorg. Chem.* **1966**, *5*, 268–277.

(30) Fortin, S.; Beauchamp, A. L. *Inorg. Chem.* **2000**, *39*, 4886–4893.

(31) Lis, T.; Jezowska-Trzebiatowska, B. *Acta Crystallogr.* **1977**, *B33*, 1248–1250.

(32) *AcornNMR NUTS*, 5.084; Acorn NMR: Livermore, CA, 1995.

(33) Bystrov, V. F. *Prog. NMR Spectrosc.* **1976**, *10*, 41–81.

Chart 2

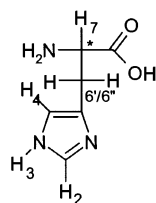
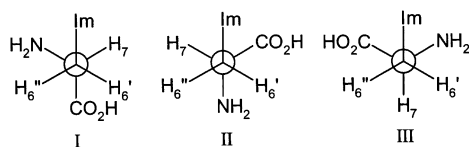
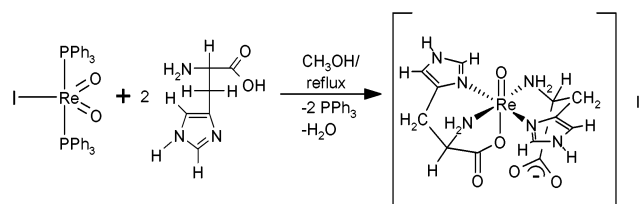


Chart 3



Scheme 2



to be roughly equal in water for free neutral histidine and for its protonated form.³⁴ If populations P_I and P_{II} are to be determined individually, the $H_{6'}$ and $H_{6''}$ signals must be assigned correctly, but even when they are not, the population P_{III} , which is the one corresponding to the tridentate histidine in the complex, can always be calculated because it depends only on the sum of the coupling constants (eq 3a). Since conformation III is imposed by the facial tridentate coordination, P_{III} should be unity. From the standard J_t (13.3 Hz) and J_g (2.4 Hz) constants proposed by Martin³⁵ for trans and gauche interactions, respectively, a value of 0.78 is obtained for P_{III} for the chloro complex and 0.74 for the bromo analogue. These departures from unity likely reflect the fairly large deviations of the coordinated ligand from the idealized conformation III.

Disubstituted Complex. Refluxing $\text{ReIO}_2(\text{PPh}_3)_2$ with 2 equiv of histidine in methanol affords a green solution containing a complex of formula $[\text{ReO}(\text{L-his-}N,N,O)(\text{L-his-}N,N)]\text{I}$ (Scheme 2), where both ligands are formally monoanionic, but one is tridentate and the other bidentate. Complexes with this stoichiometry have been reported for penicillamine (penH_2) and cysteine (cysH_2),^{13–18} where the arrangement in the equatorial plane (perpendicular to $\text{O}=\text{Re}-\text{O}$) is cis,cis (Chart 1). In our complex, the configuration is believed to be trans,trans. A cis,cis arrangement would lead to very short contacts between the H_2 atoms of the two coplanar imidazole moieties, and this geometry has not been observed so far in crystal structures of bis-histidine complexes.^{36–49}

Elemental analysis and mass spectrometry are consistent with the formula proposed. In the IR spectrum, the $\nu(\text{Re}=\text{O})$ vibration is observed as a very strong band at 960 cm^{-1} , whereas the nearby ligand bands appear weakly at 985 and 1038 cm^{-1} . Since both tridentate and bidentate ligands are present, the IR spectrum is more complex and poorly resolved. A very broad band (100 cm^{-1} at half-height), whose maximum at 1660 cm^{-1} likely corresponds to the ν_{as} mode of the coordinated carboxylate, shows distinct shoulders at 1620 cm^{-1} (free carboxylate) and 1580 cm^{-1} ($\delta(\text{NH}_2)$). By comparison with the above 1:1 complexes, the medium band at 1383 cm^{-1} is assigned to the $\nu_{\text{s}}(\text{CO}_2)$ mode of the coordinated ligand, whereas the corresponding vibration of the free carboxylate probably contributes to the band at 1433 cm^{-1} , which should also include contributions from ring stretching and/or $\rho(\text{CH}_2)$ motion. The NH_2 twisting vibration (1162 cm^{-1}) occurs at the same place as in the 1:1 complexes above, as does the well-defined band at 592 cm^{-1} , likely due to a deformation mode of the coordinated CO_2 group.

Two sets of equal intensity ^1H NMR signals (Table 2) indicate that the two nonequivalent ligands do not exchange. The signals were correlated by 2D COSY spectra. The imidazole protons are shifted downfield as above. For the aliphatic protons, one of the ligands gives rise to an AMX pattern, while accidental coincidence for $H_{6'}$ and $H_{6''}$ leads to an A_2X pattern (and a single $^3J_{\text{av}}(\text{H}_{6'}/6''-\text{H}_7)$ constant) for the other. In the latter case, by setting the sum $[^3J(\text{H}_{6'}-\text{H}_7) + ^3J(\text{H}_{6''}-\text{H}_7)]$ equal to $2[^3J_{\text{av}}(\text{H}_{6'}/6''-\text{H}_7)]$ in eq 3a, the population of rotamer III was determined to be 0.77, whereas the AMX pattern gave a P_{III} value of 0.63. In one case, the nonunity value can be ascribed as above to the distortion induced by facial tridentate coordination, but the other likely reflects that the bidentate ligand does not exist only in conformation III. At any rate, the two sets of signals cannot be assigned individually from conformational considerations. Our assignments are based on the influence of carboxylate coordination on H_7 . Since metal–carboxylate binding should reduce electron density on H_7 , the lower-field H_7 signal is assigned to the tridentate ligand. This interpretation is supported by the results obtained by Marzilli and co-workers⁵⁰ for $\text{ReO}(\text{D-pen-}S,N,O)(\text{D-penH-}S,N)$. In the latter compound, the bidentate ligand was identified unambiguously since it adopts conformation I, where the presence of a $\text{H}_7-\text{C}_7-\text{N}-\text{H}$ torsion angle of $\sim 180^\circ$ produces a large $^3J(\text{H}_7-\text{NH})$ coupling observable in the spectrum taken in DMSO. These authors found that metal coordination shifts

(34) Weinkam, R.; Jorgensen, E. C. *J. Am. Chem. Soc.* **1973**, *95*, 6084–6090.

(35) Martin, R. B. *J. Phys. Chem.* **1979**, *83*, 2404–2407.

(36) Pennington, W. T.; Cordes, A. W.; Kyle, D.; Wilson, E. W., Jr. *Acta Crystallogr.* **1984**, *C40*, 1322–1324.

(37) Candlin, R.; Harding, M. M. *J. Chem. Soc. A* **1967**, 421–423.

(38) Fuess, H.; Bartunik, H. *Acta Crystallogr.* **1976**, *B32*, 2803–2806.

(39) Harding, M. M.; Long, H. A. *J. Chem. Soc. A* **1968**, 2554–2559.

(40) Candlin, R.; Harding, M. M. *J. Chem. Soc. A* **1970**, 384–393.

(41) Thorup, N. *Acta Chem. Scand. A* **1979**, *33*, 759–763.

(42) Thorup, N. *Acta Chem. Scand. A* **1977**, *31*, 203–207.

(43) Camerman, N.; Fawcett, J. K.; Kruck, T. P. A.; Sarker, B.; Camerman, A. *J. Am. Chem. Soc.* **1978**, *100*, 2690–2693.

(44) Kretsinger, R. H.; Cotton, F. A. *Acta Crystallogr.* **1963**, *16*, 651–657.

(45) Harding, M. M.; Cole, S. J. *Acta Crystallogr.* **1963**, *16*, 643–650.

(46) Sakurai, T.; Iwasaki, H.; Katano, T.; Nakahashi, Y. *Acta Crystallogr.* **1978**, *B34*, 660–662.

(47) Herak, R.; Prelesnik, B.; Kamberi, B.; Celap, M. B. *Acta Crystallogr.* **1981**, *B37*, 1989–1992.

(48) Fraser, K. A.; Harding, M. M. *J. Chem. Soc. A* **1967**, 415–420.

(49) Forster, M.; Burth, R.; Powell, A. K.; Eiche, T.; Vahrenkamp, H. *Chem. Ber.* **1993**, *126*, 2643–2648.

(50) Hansen, L.; Xu, X. L.; Yue, K. T.; Kuklenyik, Z.; Taylor, A.; Marzilli, L. G. *Inorg. Chem.* **1996**, *35*, 1958–1966.

Table 3. ^1H NMR Chemical Shifts for the Oxo-Bridged Dimers $\{\text{Re}(\text{L-hisMe})\text{X}_2\}_2\text{O}$ (ppm)

X		H ₂	H ₃	H ₄	H _{6'} t	H _{6'}	H ₇	H _{2'}	H _{2'} t	O-CH ₃ ^a
Cl	(B)	8.370 s	12.990 s	7.305 s	2.868 dd	3.485 d	4.140 "t"	6.871 d	6.941 "t"	3.824 s
	(A)	8.126 s	13.116 s	7.465 s	3.564 "t"	3.278 d	3.455 "t"	8.904 d	5.391 "t"	3.801 s
Br	(B)	8.663 s	13.021 s	7.305 s	2.862 dd	3.473 d	4.120 "t"	6.869 d	7.172 "t"	3.803 s
	(A)	8.423 s	13.141 s	7.466 s	3.605 "t"	3.197 d	3.432 "t"	9.048 d	5.397 "t"	3.775 s

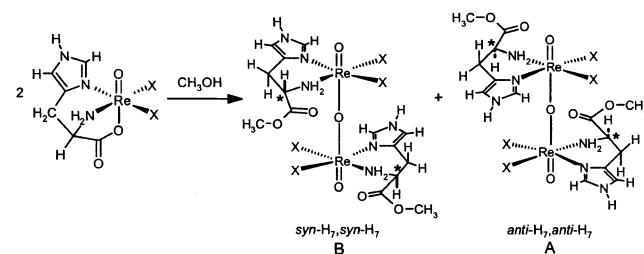
^a The methoxy signals could not be assigned individually to A or B

the H₇ proton of the tridentate ligand downfield with respect to the bidentate ligand, whose carboxylic group is not deprotonated. If carboxylate coordination makes H₇ less electron rich in the penicillamine complex even though the free carboxylic group is not deprotonated, the reduction of electron density should be greater here, where the free carboxylate group of the bidentate ligand is anionic. Thus, our lower-field H₇ signal, and those of the correlated protons, can safely be assigned to the tridentate histidine.

The predominance of conformation III for the N,N'-bidentate histidine in $[\text{ReO}(\text{L-his})_2]^+$ is not unreasonable, since conformations I and III are equally represented in crystal structures (Table S-2, Supporting Information). Considering that the preference of ReO (D-pen-S,N,O)(D-penH-S,N) for conformation I was noted in DMSO, we considered the possibility that the CD₃OD solvent used here could be the factor stabilizing conformation III. However, spectral data for the related ReO(L-cys-S,N,O)(L-cysH-S,N) compound (Supporting Information) indicated that the bidentate ligand retains conformation I in both DMSO and CD₃OD. Therefore, the different conformation for the histidine complex must be due to intrinsic features of the molecule, such as the different flexibility of the equatorial chelate ring, which is five-membered in ReO(pen)(penH) and ReO(cys)(cysH), but six-membered in $[\text{ReO}(\text{L-his})_2]^+$. On the other hand, electrostatic and hydrogen-bonding interactions should differ appreciably, since the carboxylate group of L-histidine is anionic, but protonated in the complexes of the S-containing amino acids.^{34,35,51}

Our many attempts to obtain crystals for X-ray work failed. Slow evaporation of the methanol solution afforded an oily residue. Vapor diffusion of ether into a methanol solution or addition of a large anion like BPh₄⁻ gave no precipitate. Crystallization from aqueous solutions was ruled out since $[\text{ReO}(\text{L-his})_2]^+$ decomposed.

Oxo-Bridged Dimers. When left in methanol, the mono-substituted complex $\text{ReOCl}_2(\text{L-his})$ produced a light-green precipitate, insoluble in most common solvents except DMSO and DMF. The reaction could be accelerated by addition of HCl, but ^1H NMR spectroscopy indicated that side-products formed. The color and insolubility of the solid, as well as the very strong multicomponent IR band at $\sim 695\text{ cm}^{-1}$ (Re-O-Re stretch), suggested an oxo-bridged dimer (Scheme 3).⁵² The ^1H NMR spectrum in DMSO (Table 3) showed a sharp signal at ca. 3.8 ppm for a methyl-ester group, indicating that the histidine ligand had esterified. The presence of an ester group was also supported by the strong $\nu(\text{C}=\text{O})$ band occurring at high wavenumber (1712 cm^{-1})

Scheme 3

and a weak band at 1021 cm^{-1} for the ester $\nu(\text{O}-\text{CH}_3)$ mode.⁵³ The remainder of the IR spectrum was not very different from the one of $\text{ReOCl}_2(\text{L-his})$. Elemental analysis was consistent with the compound being $\{\text{OReCl}_2(\text{L-hisMe})\}_2(\mu\text{-O})$. The corresponding bromo complex was not isolated on a preparative scale, but considering the very close similarity of their NMR spectra, the chloro and the bromo compounds must have the same structure.

The NMR spectrum contained two sets of histidine signals, which could be consistent with the presence of two non-equivalent ligands in the molecule. However, the crystallographic work on $\{\text{OReBr}_2(\text{L-hisMe})\}_2(\mu\text{-O})$ (see below) showed that the compound was an uncommon stoichiometric mixture (1:1 ratio) of the diastereoisomers illustrated in Scheme 3, arranged in a perfectly ordered manner. These diastereoisomers will be labeled syn or anti, depending on the orientation of H₇ (on the chiral carbon *) relative to the Re=O bond. Each isomer possesses a C₂ axis through the central oxygen and perpendicular to the O=Re-O-Re=O backbone. In agreement with the two halves of the molecule being equivalent for each isomer, two sets of signals are observed. The absence of extra signals shows that no other isomer is present. The signals belonging to each set were correlated from a 2D COSY spectrum. Selective irradiation was also used to unravel the complex 3.1–3.6 ppm region, where several signals overlap the residual water peak. The imidazole N-H protons occur as sharp signals at ~ 13 ppm, whereas the four ring C-H protons give rise to high-intensity singlets in the 7–9 ppm range. Details on the assignments of the aliphatic protons are provided as Supporting Information.

Each coherent set of signals is tentatively assigned to one of the two isomers observed in the crystals by assuming that a certain conformational freedom exists in solution. Indeed, although the solid-state conformation is assumed to be predominant in solution, rotation of the two halves of the molecule about the O=Re-O-Re=O axis in solution likely brings momentarily the two histidine ligands above one another. In this transitory structure, protons pointing toward

(51) Martin, R. B.; Mathur, R. *J. Am. Chem. Soc.* **1965**, *87*, 1065–1070.

(52) Fortin, S.; Beauchamp, A. L. *Inorg. Chim. Acta* **1998**, *279*, 159–164.

(53) Wilmschurst, J. K. *J. Mol. Spectrosc.* **1957**, *1*, 201–215.

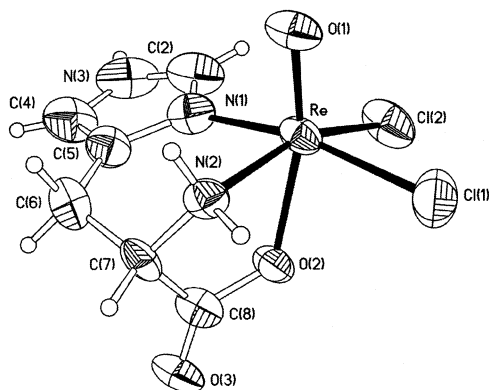


Figure 1. ORTEP drawing of $\text{ReOCl}_2(\text{L-his-}N,N,O)$. Ellipsoids correspond to 40% probability.

the inside of the molecule should be selectively shielded by the anisotropic effect of the imidazole ring. In the *anti-H₇,anti-H₇* isomer, both H₇ protons are pointing toward the center of the molecule. Therefore, the set of signals A (Table 3) is assigned to this isomer, since H₇ is more shielded (3.45 ppm) than in the other isomer (4.14 ppm, set B), where the H₇ protons are syn to the Re=O bond and pointing outward. This assumption also holds for the H_{6'} protons, which lie trans to H₇. As expected, they exhibit the opposite effect: the H_{6'} protons in the *syn-H₇,syn-H₇* isomer are observed upfield (2.87 ppm, set B) from those of the *anti-H₇,anti-H₇* isomer (3.56 ppm, set A). This simple pattern is not followed by the NH₂ signals: although the H_{2'} protons in the *syn-H₇,syn-H₇* isomer are anti to the Re=O bond, they are less shielded (6.94 ppm) than those of the *anti-H₇,anti-H₇* isomer (5.39 ppm). However, the N–H resonances are expected to be more sensitive to the nearby Re=O bond than to the more remote imidazole moiety in the other ligand.

Crystal Structures. $\text{ReOCl}_2(\text{L-his-}N,N,O)$ (1). The crystals contain the distorted octahedral molecule shown in Figure 1, where the histidine ligand is N,N,O-tridentate. The NH₂ group, a non-deprotonated imidazole, and two chloro ligands occupy the equatorial plane, whereas a carboxylate oxygen is located trans to the Re=O bond in the axial direction. This trans O=Re–O(carboxylate) arrangement has been observed in various systems, such as $\text{ReO}(\text{pen-}S,N,O)(\text{penH-}S,N)$,¹⁴ $\text{ReO}(\text{cys-}S,N,O)(\text{cysH-}S,N)$,¹⁵ their methyl ester derivatives^{16–18} (for the tridentate ligand), and cysteine derivatives such as ethylene-di-L-cysteine (LL-ECH₆).⁵⁴ An exception is the *syn-ReO(DL-ECH₃)* compound, where the carboxylate oxygen lies in the equatorial plane and an NH₂ group is trans to the Re=O bond.⁵⁵

This structure is the first example of a transition metal M(V) complex with histidine. A related vanadium(IV) compound $[\text{NMe}_4][\text{VO}(\text{L-his-}N,N,O)(\text{NCS})_2]$ was obtained, where the same arrangement for the histidine ligand was noted.⁵⁶ Selected bond lengths are listed in Table 4. The Re=O distance (1.660(6) Å) compares well with those

Table 4. Bond Lengths (Å) for the Complexes

	Re=O	Re–O	Re–X(1)	Re–X(2)	Re–NH ₂	Re–N(Im)
1	1.660(6)	2.081(6)	2.351(3)	2.334(2)	2.146(6)	2.099(8)
2	1.666(8)	2.093(7)	2.497(1)	2.482(1)	2.171(9)	2.108(10)
4	1.677(12)	1.913(1)	2.577(2)	2.507(3)	2.200(13)	2.099(13)
	1.715(15)	1.912(1)	2.588(2)	2.522(3)	2.116(15)	2.100(16)

obtained for the complexes with penicillamine, cysteine, and their derivatives.^{14–18} The Re–Cl(1) distance (2.351(3) Å) is slightly longer than Re–Cl(2) (2.334(2) Å), probably because Cl(1) participates in hydrogen bonding, but both distances are within the accepted range.⁵⁷ The Re–NH₂ bond is ~0.05 Å longer than the Re–N(Im) bond, in agreement with the literature data for complexes with amino acids (mean $\text{Re}^V\text{–N} = 2.188$ Å, $\sigma = 0.032$ Å, 20 data)^{15,17,18,58} and imidazoles (mean $\text{Re}^V\text{–N} = 2.124$ Å, $\sigma = 0.016$ Å, 35 data).^{59–64}

The angles listed in Table S-5 (Supporting Information) show that the octahedron is severely distorted. The general displacement of the “equatorial” ligands away from the Re=O bond opens all the cis O=Re–L angles (mean 98.0°), reducing the trans angles below 180° and the cis angles below 90° in this plane. This distortion, which is common in mono-oxo complexes, affects particularly the chloro ligands (O=Re–Cl = 99.4(3)° and 108.7(2)°) and raises the Re atom 0.315(3) Å above the ReCl_2N_2 plane toward the oxo ligand. Coordination of the carboxylate group introduces further distortion. The five-membered ring imposes a small H₂N–Re–O bite angle (73.2(2)°) whose effect is felt mainly in the O=Re–O moiety deviating from linearity (162.8(3)°). Similar distortions are observed in the penicillamine and cysteine systems.^{14,16–18}

Coordination of the imidazole moiety takes place almost exactly along the expected lone pair direction, as evidenced from the C(2)–N(1)–Re and C(5)–N(1)–Re angles being very close (126.0(8)° and 127.2(6)°, respectively). The imidazole ring is rotated ~22° with respect to the “equatorial” N₂Cl₂ plane. The departure of 0.10(1) Å of the Re atom from the mean plane through the imidazole ring is significant, but relatively small. The strain introduced by the tridentate coordination in the aliphatic part is detected only in the carboxylate region, where the C(7)–C(8)–O(2) angle in the chelate ring (111.4(7)°) is ~5° below the value generally found in metal complexes (Table S-3, Supporting Information), whereas the external C(7)–C(8)–O(3) angle (125.0(9)°) is increased by the same extent.

The C(5)–C(6)–C(7)–N(2) and C(5)–C(6)–C(7)–C(8) torsion angles (Table 5) of 67(1)° and –52(1)°, respectively,

(57) Wilson, A. J. C. E. *International Tables for X-Ray Crystallography*, 2nd ed.; Kluwer Academic Publishers: Dordrecht, The Netherlands, 1995; Vol. C.

(58) Melian, C.; Kremer, C.; Suescun, L.; Mombro, A.; Mariezcurrena, R.; Kremer, E. *Inorg. Chim. Acta* **2000**, *306*, 70–77.

(59) Alessio, E.; Zangrando, E.; Iengo, E.; Macchi, M.; Marzilli, P. A.; Marzilli, L. G. *Inorg. Chem.* **2000**, *39*, 294–303.

(60) Pearson, C.; Beauchamp, A. L. *Acta Crystallogr.* **1994**, *C50*, 42–44.

(61) Lebus, A. M.; Young, J. M. C.; Beauchamp, A. L. *Can. J. Chem.* **1993**, *71*, 2070–2078.

(62) Bélanger, S.; Beauchamp, A. L. *Inorg. Chem.* **1996**, *35*, 7836–7844.

(63) Bélanger, S.; Beauchamp, A. L. *Inorg. Chem.* **1997**, *36*, 3640–3647.

(64) Hansen, L.; Alessio, E.; Iwamoto, M.; Marzilli, P. A.; Marzilli, L. G. *Inorg. Chim. Acta* **1995**, *240*, 413–417.

(54) Marzilli, L. G.; Banaszczyk, M. G.; Hansen, L.; Kuklenyik, Z.; Cini, R.; Taylor, A. *Inorg. Chem.* **1994**, *33*, 4850–4860.

(55) Hansen, L.; Lipowska, M.; Taylor, A.; Marzilli, L. G. *Inorg. Chem.* **1995**, *34*, 3579–3580.

(56) Xiaoping, L.; Kangjing, Z. *J. Crystallogr. Spectrosc. Res.* **1986**, *16*, 681–685.

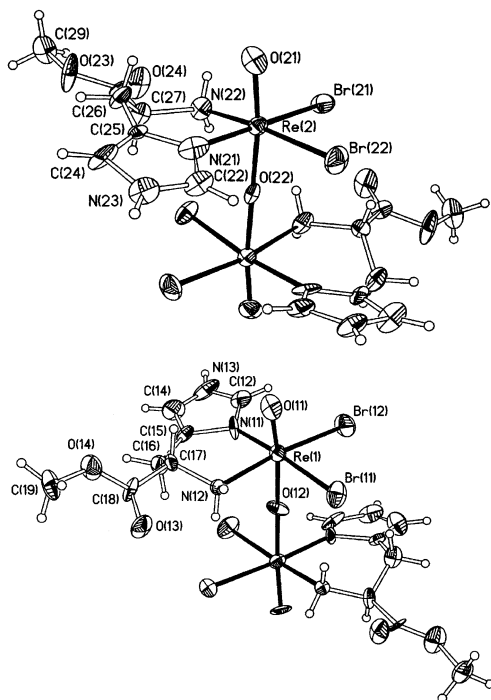


Figure 2. ORTEP drawing of the asymmetric unit consisting of two independent $\{\text{OREBr}_2(\text{L-hisMe-}N,N)\}_2\text{O}$ molecules, both lying on crystallographic 2-fold axes. Ellipsoids correspond to 40% probability.

Table 5. Conformation of the Histidine Ligand in the Complexes

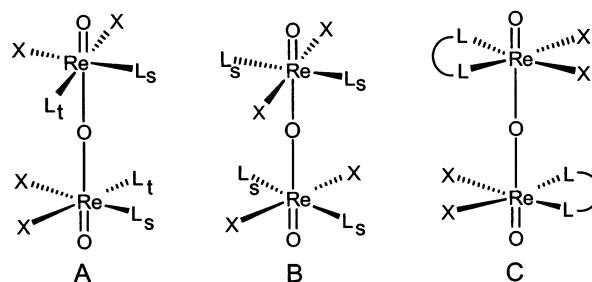
	coord	C(5)–C(6)–C(7)–N(2)	C(5)–C(6)–C(7)–C(8)	conf
1	N,N,O	67(1)	–52(1)	III
2	N,N,O	69(1)	–46(2)	III
4	N,N	–76(2)	165(1)	I
	N,N	–66(2)	171(1)	I

are close to the ideal values of $+60^\circ$ and -60° , typical of conformation III (Chart 3). The remaining torsion angles (Table S-4, Supporting Information) do not differ greatly from those of other histidine complexes, in agreement with the conformational constraints imposed by tridentate coordination. The carboxylate plane is displaced by $\sim 20^\circ$ from the eclipsed orientation with respect to the CH-NH_2 bond and nearly perpendicular to the $\text{C(Im)-CH}_2\text{-CH}$ backbone (dihedral angle of $\sim 80^\circ$). Besides the complex molecules, the unit cell contains water molecules O(4) lying on crystallographic 2-fold axes. They act as donors in hydrogen bonds with the free carboxylate oxygens O(3) and as acceptors from the NH_2 groups. Details on hydrogen bonding are given in Table S-6 (Supporting Information).

In the isostructural $\text{ReOBr}_2(\text{L-his-}N,N,O)$ compound (crystal 2), the Re-Br bonds are of normal length⁵⁷ and no particular structural differences are noted with respect to the chloro analogue.

$\{\text{ORE}(\text{L-hisMe})\text{Br}_2\}_2\text{O}$ (Crystal 4). The asymmetric unit of the monoclinic cell is shown in Figure 2. It consists of two linear oxo-bridged dinuclear $\{\text{ORE}(\text{L-hisMe})\text{Br}_2\}_2\text{O}$ molecules, each lying on a crystallographic 2-fold axis. In both cases, the metal environment is approximately octahedral. The equatorial plane includes two Br ligands and a bidentate histidine bonded via the amino group and an imidazole nitrogen, whereas the carboxylate group is me-

Chart 4



thylated. The two molecules differ by the relative orientations of the histidine ester ligands.

Selected distances are listed in Table 4, whereas angles are provided in Table S-5. Considering that the superlattice effect in this structure (see Experimental Section) leads to relatively large esd's, which are probably somewhat underestimated, the Re-N distances do not differ significantly from those of $\text{ReOBr}_2(\text{L-his-}N,N,O)$. The Re=O (mean 1.69 Å) and bridging Re-O (mean 1.913 Å) distances are typical of the O=Re-O-Re=O backbone.^{30,52,60,65} One of the Re-Br bonds in each molecule (mean 2.58 Å) is ~ 0.07 Å longer than the other, probably because it is the only one taking part in hydrogen bonding. The angles around the Re atoms are closer to ideality than in the above monomeric bromo complex, because the large distortion produced by the five-membered chelate ring involving the carboxylate is no longer present. The O=Re-O , N(Im)-Re-Br(1) , and $\text{NH}_2\text{-Re-Br(2)}$ units are now closer to linearity ($170.5/173.9/172.4^\circ$ vs $163.5/167.4/160.9^\circ$, respectively). With a central Re-O-Re angle of 178.4° (mean), the O=Re-O-Re=O backbone can be regarded as essentially linear. A small distortion results from the Re=O bond repelling the adjacent ligands: the $\text{O=Re-L}_{\text{cis}}$ angles (mean 92.7°) tend to be slightly greater than the $\text{O-Re-L}_{\text{cis}}$ angles (mean 87.2°), which corresponds to a displacement of the Re atom by ~ 0.10 Å above the N_2Br_2 plane.

Although various oxo-bridged dimers of the type $\{\text{ORE-L}_2\text{X}_2\}_2\text{O}$ are known for $\text{X} = \text{Cl}$, this is the first example of a bromo derivative. Unless it is constrained by a bridging ligand like N,N' -dimethylbiimidazole,³⁰ the O=Re-O-Re=O backbone is essentially linear whether the ligand arrangement in the equatorial plane is cis or trans. With monodentate ligands, a cis configuration has been observed for $\{\text{ORECl}_2(\text{py})_2\}_2\text{O}$,⁶⁵ $\{\text{ORECl}_2(3,5\text{-Me}_2\text{pzH})_2\}_2\text{O}$,⁶⁶ $\{\text{ORECl}_2(\text{Me}_3\text{Bzm})_2\}_2\text{O}$,⁶⁷ $\{\text{ORECl}_2(\text{Me}_3\text{Bzm})(\text{py})\}_2\text{O}$, and $\{\text{ORECl}_2(\text{Me}_3\text{Bzm})(3,5\text{-lut})\}_2\text{O}$.⁵⁹ The conformation found in these complexes has been analyzed in detail by Lock and Turner.⁶⁵ The dihedral angles between the heterocyclic ligands L and the ReCl_2L_2 plane are $37\text{--}58^\circ$, to minimize short contacts around the Re=O and Re-Cl bonds. The ORECl_2L_2 units are also rotated $23\text{--}32^\circ$ about the Re-Re axis away from an eclipsed conformation (Chart 4A): this arrangement avoids short contacts between ligands L in different halves

(65) Lock, C. J. L.; Turner, G. *Can. J. Chem.* **1978**, *56*, 179–188.

(66) Dahmann, G. B.; Enemark, J. H. *Inorg. Chem.* **1987**, *26*, 3960–3962.

(67) Marzilli, L. G.; Iwamoto, M.; Alessio, E.; Hansen, L.; Calligaris, M.; Bandoli, G.; Dolmella, A.; Gerber, T. I. A.; Dupreez, J. G. H.; Kemp, H. *J. Am. Chem. Soc.* **1994**, *116*, 815–816.

Oxorhenium(V) Complexes

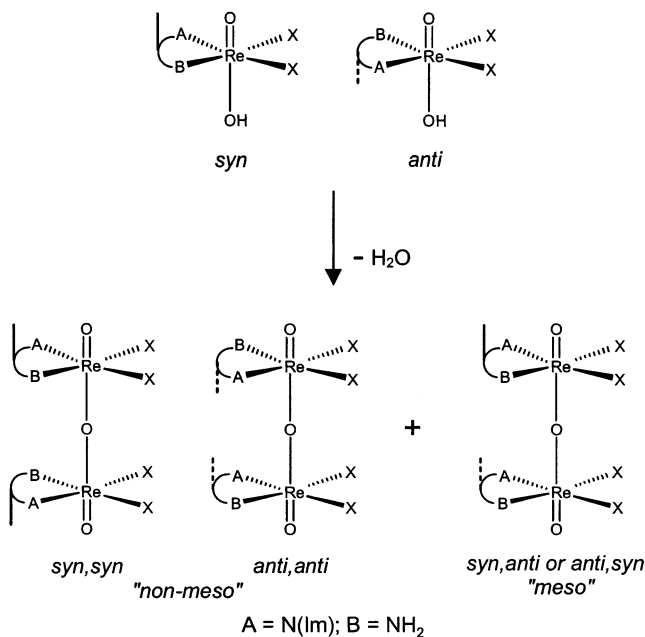
of the dimer and allows some stacking interaction to take place between ligands L_s , leaving the other pair (L_t) in transoid positions.

The $\{\text{OReCl}_2(1\text{-MeIm})_2\}_2\text{O}^{60}$ and $\{\text{OReCl}_2(\text{py})_2\}_2\text{O}^{52}$ complexes containing a trans arrangement of the monodentate ligands (Chart 4B) have also been characterized. Again, the ligand makes dihedral angles of $37\text{--}51^\circ$ with the equatorial plane. The OReCl_2N_2 units are rotated away from the eclipsed arrangement, and the $L_s\text{-Re-Re-L}_s$ torsion angles of $26\text{--}29^\circ$ compare well with those of the cis,cis complexes described above (Chart 4A). This conformation allows stacking interactions to occur between the two pairs of heterocyclic ligands.

With bidentate ligands, the configuration is necessarily cis (Chart 4C). Four examples are known: $\{\text{OReCl}_2(\text{en})\}_2\text{O}^{68}$, $\{\text{OReCl}_2(\text{biimH}_2)\}_2\text{O}^{30}$, $\{\text{OReCl}_2(1,8\text{-diacetoxy-3,6-dithiaoctane})\}_2\text{O}^{69}$ and $\{\text{OReCl}_2(5,8\text{-dithiadodecane})\}_2\text{O}^{70}$. For the complexes with ethylenediamine and biimidazole, the bridging oxygen atom sits on an inversion center, so that a perfectly eclipsed conformation is observed. The two thiolate molecules do not lie on a symmetry element, but the deviations from eclipsed conformations are small (torsion angles of 177.2° and 166.1°). In contrast with the other oxo-bridged dimers, the O=Re-O-Re=O backbone shows a significant deviation from linearity in the latter two complexes ($\text{Re-O-Re} = 166.5^\circ$ (mean) and $\text{O=Re-O} = 163.2^\circ$ (mean)).^{69,70}

Crystal **4** can be regarded as belonging to the last type, with two noticeable differences: the two donor atoms are different and the amino acid contains a chiral center. These peculiarities increase the number of possible isomers. An achiral $L\text{-L}'$ bidentate ligand should produce a meso isomer (A donors above one another, Scheme 4) and a pair of enantiomers (A above B and vice versa). The arrangement of donor atoms observed here for the two nonequivalent molecules in the asymmetric unit corresponds to the non-meso pair. However, since the ring includes an asymmetric carbon and the compound was prepared from L-histidine, these two species are actually diastereoisomers, which are designated as syn,syn or anti,anti, according to whether the H_7 proton on the chiral center is syn or anti with respect to the Re=O bond. Each of these species is chiral, but the opposite enantiomer is not formed, since it would contain D-histidine. Nevertheless, the difference between the syn,syn and the anti,anti isomers results almost exclusively from the position of the methylene group above or below the mean plane through the chelate ring. This introduces only a very minor effect on the overall van der Waals envelope, and the molecule adopts a quasi-centrosymmetric arrangement in the crystal (corresponding to space group $C2/c$), as if they were actually pairs of non-meso enantiomers devoid of asymmetric carbons. Careful interpretation of the X-ray data in spite of the problems created by this superlattice allowed us to show

Scheme 4. Coupling of Two Oxo-Hydroxo Tautomeric Units To Yield the Three Dinuclear Diastereoisomers^a



^a For simplicity, eclipsed conformations are used in the diagrams.

that equal amounts of diastereoisomers syn,syn and anti,anti are actually present. In both cases, the bridging oxo atom lies on a crystallographic 2-fold axis relating the two OReBr_2 ($L\text{-hisMe}$) units, which adopt the eclipsed conformation of Chart 4C (torsion angle $\sim 180^\circ$) observed for other bidentate ligands.

In the solid state, N,N' -bidentate histidine adopts conformations I or III (Table S-2). In the present case, the torsion angles of Table 5 show that the ligand adopts conformation I, for which the $\text{C}(5)\text{-C}(6)\text{-C}(7)\text{-N}(2)$ and $\text{C}(5)\text{-C}(6)\text{-C}(7)\text{-C}(8)$ angles should ideally be -60° and 180° , respectively. In this conformation, one of the H_6 protons lies trans to the H_7 proton on the chiral carbon atom and to one of the NH_2 protons. The above NMR data could be rationalized in terms of this conformation, thereby showing that the solid-state structure is retained, or at least predominant, in solution. The imidazole ring makes angles of $8.2(3)^\circ$ and $17.1(5)^\circ$ with the "equatorial" Br_2N_2 plane for molecules 1 and 2, respectively. Other torsion angles are listed in Table S-4. Since the carboxylate group is not coordinated and pointing away from the metal center, its orientation is not greatly restricted. In the syn,syn isomer, the CO_2 unit is roughly coplanar with the CH-NH_2 bond ($\text{N}(2)\text{-C}(7)\text{-C}(8)\text{-O}(3)$ angle of $-4(2)^\circ$), whereas in the anti,anti isomer, it is rotated by $\sim 25^\circ$ as in the monodentate complexes. These conformations are controlled to a certain extent by intermolecular hydrogen bonding of the amino protons.

In each molecule, two symmetry-equivalent $\text{N-H}\cdots\text{Br}$ hydrogen bonds are formed by an NH_2 group and a Br ligand from the other half of the dimer. The $\text{N}\cdots\text{Br}$ separation of 3.41 \AA (Table S-7, Supporting Information) is close to the typical value of 3.37 \AA .⁷¹ In the syn,syn isomer (molecule

(68) Glowiak, T.; Lis, T.; Jezowska-Trzebiatowska, B. *Bull. Acad. Pol. Sci., Ser. Sci. Chim.* **1972**, *20*, 199–207.

(69) Pietzsch, H. J.; Reisinger, M.; Spies, H.; Leibnitz, P.; Johannsen, B. *Chem. Ber.* **1997**, *130*, 357–361.

(70) Pietzsch, H. J.; Spies, H.; Leibnitz, P.; Reck, G. *Polyhedron* **1995**, *14*, 1849–1853.

(71) Pimentel, G. C.; McClellan, A. L. *Annu. Rev. Phys. Chem.* **1971**, *22*, 347–385.

1), the N–H bond is parallel to the O=Re–O–Re=O backbone (H–N–Re–(μ -O) torsion angle of 6°) and a nearly linear hydrogen bond results (N–H–Br angle = 169°). The geometry is less favorable in the anti,anti isomer, since the N–H bond lies closer to the plane of the chelate ring (H–N–Re–(μ -O) angle = 34°) and the hydrogen bond deviates from linearity (N–H–Br = 142°). Nevertheless, these interactions seem to be strong enough to make the Re–Br(1) distances longer than Re–Br(2), and they likely contribute to stabilize the observed conformations.

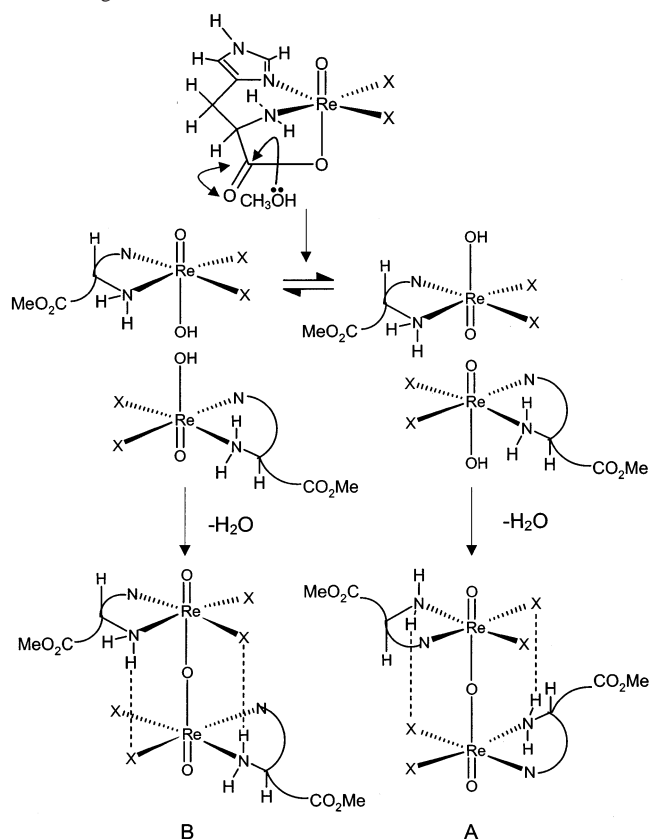
Discussion

In the reaction with $\text{ReOX}_3(\text{OPPh}_3)(\text{Me}_2\text{S})$, the first histidine is introduced into the coordination sphere as an anionic tridentate ligand with the carboxylato group trans to the Re=O bond. In related systems,⁵² the good-leaving Me_2S ligand was found to be displaced first and the initial step of the present reaction is probably its substitution by the imidazole ring. Since the carboxylate is more nucleophilic than the still protonated $-\text{NH}_3^+$ group, the next best leaving group, OPPh_3 , could then be displaced by the carboxylate, leading to an intermediate with the very stable *trans*-O=Re–O unit. Finally, the reduced positive charge of this intermediate and the cooperative effect of the already bidentate-coordinated ligand would assist the elimination of the chloro ligand as HCl and the coordination of the amino group.

A disubstituted complex is also obtained, in which the second histidine enters as an N,N-bidentate ligand, while its carboxylate group remains free. In this respect, histidine behaves like cysteine and penicillamine, except that the configuration in the equatorial plane is *cis,cis* for the S-containing amino acids and *trans,trans* for L-histidine. In methanol, the 1:1 complex condenses to an oxo-bridged dinuclear species with concomitant esterification of the carboxylate groups. It is interesting to note that, according to our NMR spectra and crystal structure determination, this process leads to equal amounts of the two non-meso diastereoisomers, whereas the third meso-type species is not observed.

These peculiarities are consistent with the mechanism given in Scheme 5, where the nucleophilic attack of methanol would first produce a tautomeric mixture of two oxo-hydroxo species containing histidine as the methyl ester. Condensation of two such oxo-hydroxo units with water elimination would then lead to species containing the O=Re–O–Re=O backbone. On this basis, a statistical mixture of the three stereoisomers shown in Scheme 4 should form, but only the two non-meso species were actually observed in the solid state and in solution. A possible explanation for this specificity is suggested by the crystal structure, where a pair of complementary N–H \cdots Br hydrogen bonds are present between the two halves of both molecules A and B. Molecular models show clearly that such a pair of hydrogen bonds can hold two oxo-hydroxo fragments properly oriented to lead to isomer A by water elimination, as shown in Scheme 5. Similarly, two oxo-hydroxo fragments differently oriented could generate isomer

Scheme 5. Proposed Mechanism for the Formation of the Oxo-Bridged Dimers^a



^a In pathway A, each oxo-hydroxo species must be rotated by 180° around an axis bisecting the X–Re–X angle in order to bring the hydroxo groups in a suitable orientation for condensation.

B. However, no such pair of hydrogen bonds could be established between fragments that would end up as the meso isomer. Therefore, a pair of hydrogen bonds could help stabilize the two forms observed here, by favorably orienting the two monomers for water elimination, thereby introducing specificity in the condensation process.

This work shows that histidine binds strongly to the Re(V) center and can produce a tridentate complex. This suggests that this residue could efficiently act as a binding group to label peptides with rhenium. Work is underway to determine if a terminal histidine residue in a peptide retains a high affinity for rhenium in spite of the amide oxygen being less basic than the carboxylate.

Acknowledgment. The financial support of the Natural Sciences and Engineering Research Council of Canada is gratefully acknowledged.

Supporting Information Available: Detailed ^1H NMR signal assignments for $\{\text{OReX}_2(\text{L-hisMe})\}_2(\mu\text{-O})$, ^1H NMR data for $\text{ReO}(\text{L-cys-S},\text{N},\text{O})(\text{L-cysH-S},\text{N})$, IR data for the four complexes, X-ray crystallographic files in CIF format, selected bond angles and detail on hydrogen bonds for **1**, **2**, and **4**, figure of crystal packing for **4**, and distances, angles, and torsion angles in crystal structures of histidine metal complexes. This material is available free of charge via the Internet at <http://pubs.acs.org>.

IC025809M